

RESEARCH ARTICLE

α -Catenin stabilises Cadherin–Catenin complexes and modulates actomyosin dynamics to allow pulsatile apical contraction

Jaime Jurado¹, Joaquín de Navascués² and Nicole Gorfinkiel^{1,*}**ABSTRACT**

We have investigated how cell contractility and adhesion are functionally integrated during epithelial morphogenesis. To this end, we have analysed the role of α -Catenin, a key molecule linking E-Cadherin-based adhesion and the actomyosin cytoskeleton, during *Drosophila* embryonic dorsal closure, by studying a newly developed allelic series. We find that α -Catenin regulates pulsatile apical contraction in the amnioserosa, the main force-generating tissue driving closure of the embryonic epidermis. α -Catenin controls actomyosin dynamics by stabilising and promoting the formation of actomyosin foci, and also stabilises DE-Cadherin (*Drosophila* E-Cadherin, also known as Shotgun) at the cell membrane, suggesting that medioapical actomyosin contractility regulates junction stability. Furthermore, we uncover a genetic interaction between α -Catenin and Vinculin, and a tension-dependent recruitment of Vinculin to amnioserosa apical cell membranes, suggesting the existence of a mechano-sensitive module operating in this tissue.

KEY WORDS: α -Catenin, DE-Cadherin, Oscillation, Apical contraction, Actomyosin, Vinculin, Morphogenesis

INTRODUCTION

Epithelial morphogenesis, the coordinated set of cell movements that generates biological shape, requires the integration of the activity of the actomyosin cytoskeleton with cadherin-based junctions, allowing the coordination of local cell shape changes into tissue-level deformations (Heisenberg and Bellaiche, 2013). There is ample evidence that the actomyosin cytoskeleton influences adhesion dynamics, and conversely, that adherens junctions influence the functioning of the contractile machinery, suggesting that there are complex biochemical and mechanical feedback mechanisms that are only starting to be elucidated (Lecuit and Yap, 2015; Yap et al., 2015).

E-Cadherin-based junctions are fundamental adhesion centres of epithelial cells and are physically linked to the actomyosin cytoskeleton. α -Catenin is a key protein in maintaining this link and acts by binding to E-Cadherin, through its interaction with β -catenin, and to F-actin directly, through its C-terminal domain. Although biochemical studies had challenged the notion that the Cadherin–Catenin complex binds directly to F-actin (Drees et al., 2005; Yamada et al., 2005), recent experimental findings using an optical trap assay have shown that strong and stable bonds between

the Cadherin–Catenin complex and an actin filament form under force, probably requiring a conformational change of α -Catenin (Buckley et al., 2014). Force-dependent conformational changes in vertebrate α E-Catenin (also known as CTNNA1) regulate its binding to Vinculin, an actin-binding protein, and reinforce intercellular adhesion (Kim et al., 2015; le Duc et al., 2010; Yao et al., 2014; Yonemura et al., 2010). Moreover, using a fluorescence resonance energy transfer (FRET) tension sensor, it has been shown that the actomyosin cytoskeleton exerts tensile forces on E-Cadherin in an α -Catenin-dependent manner (Borghi et al., 2012). Taken together, these observations show that α -Catenin is a key mechanosensory protein transmitting actomyosin cytoskeletal tension to the cell membrane.

In spite of these observations, how α -Catenin contributes to the dynamic remodelling of cells in the context of tissue morphogenesis has remained less explored. Recently, detailed structure–function analysis of α -Catenin in *Drosophila* has shown that, *in vivo*, the persistent physical linkage between the Cadherin–Catenin complex and the actin cytoskeleton is absolutely required for α -Catenin function (Desai et al., 2013). α -Catenin can bind to actin through its C-terminal actin-binding domain. For example, in the actin-binding domain of *C. elegans* α -Catenin, discrete regions and specific residues have been shown to modulate attachment to junctional actin during epidermal morphogenesis (Maiden et al., 2013). However, there is also evidence that the interaction of α -Catenin with other actin-binding proteins such as Formin and EPLIN (also known as LIMA1) can provide an indirect link to the actin cytoskeleton that is likely to contribute to particular aspects of α -Catenin function during morphogenesis (Huvneers and de Rooij, 2013; Maiden and Hardin, 2011). These results suggest that there are complex interactions between α -Catenin, other actin-binding proteins and the actomyosin cytoskeleton during morphogenesis that remain to be elucidated.

To have a better understanding of the role of α -Catenin during morphogenesis, we have analysed its function during dorsal closure, a morphogenetic process that is being widely used as a model system to understand the interplay between cell activity and mechanics (Gorfinkiel et al., 2011). After germband retraction, the dorsal side of the *Drosophila* embryo is covered by an extra-embryonic epithelium, the amnioserosa. During dorsal closure, the amnioserosa contracts through the apical contraction of its individual cells, and the lateral epidermis converges towards the dorsal midline, to eventually generate epidermal continuity (Jacinto et al., 2002; Kiehart et al., 2000). Apical contraction in amnioserosa cells is pulsatile, driven by periodic contractions of the actomyosin cytoskeleton at the apical surface of cells (Blanchard et al., 2009; David et al., 2013; Martin et al., 2009; Solon et al., 2009). The mechanism underlying the emergence of this oscillatory activity and how it is stabilised to give rise to effective cell shape changes has been a matter of intense research during the last years (Gorfinkiel, 2016). Several studies have revealed that the control of Myosin

¹Centro de Biología Molecular “Severo Ochoa”, CSIC-UAM, Cantoblanco, Madrid 28049, Spain. ²European Cancer Stem Cell Research Institute, School of Biosciences, Cardiff University, Cardiff CF24 4HQ, UK.

*Author for correspondence (ngorfinkiel@cbm.csic.es)

 N.G., 0000-0002-6847-6721

phosphorylation is fundamental for the appearance of actomyosin oscillations and for its proper dynamics (Munjal et al., 2015; Vasquez et al., 2014). In contrast, the contribution of adhesion to pulsatile actomyosin activity has been less explored, even though the engagement of the medial actomyosin cytoskeleton to the membrane is required for cell shape changes to occur. Although it has been proposed that apical contraction is triggered by the engagement of a link between cell–cell junctions and an intrinsically contractile actomyosin network (Roh-Johnson et al., 2012), the molecular basis of this link remains unknown. Thus, investigating the nature and dynamics of the link between the actomyosin cytoskeleton and the cell membrane is essential to understand the mechanisms driving apical contraction.

We have generated an allelic series for α -Catenin and investigated the requirements for α -Catenin during *Drosophila* dorsal closure, and in particular, in the contraction of the amnioserosa. We show that α -Catenin is required for the actomyosin dynamics and the stabilisation of E-Cadherin at the cell membranes. Furthermore, we find that Vinculin has both α -Catenin-dependent and -independent functions, and that Vinculin is recruited to the apical cell membrane of amnioserosa cells in a Myosin-II-dependent manner. Taken together, our results suggest that both α -Catenin and Vinculin are part of a mechano-sensitive module operating in amnioserosa cells.

RESULTS

Mutations in the actin-binding domain of α -Catenin give rise to loss-of-function alleles

α -Catenin is a multi-domain protein composed of three main functional modules: (1) an N-terminal VH1 domain, containing the Armadillo-binding and the homodimerisation domains, (2) a central region, containing a Vinculin-binding site (VBS) and the VH2 domain, which can undergo conformational changes in response to actomyosin-generated tension and, (3) a C-terminal domain VH3 that binds to F-actin (Fig. 1B). To study α -Catenin function in the context of a developing organism, we carried out a chemical mutagenesis in a background bearing a proximal FRT site (see Materials and Methods) and isolated four alleles for α -Catenin (α -Cat) (Fig. 1A,B). Although several mutant constructs for *Drosophila* α -Cat have been generated (Desai et al., 2013), their functional analysis requires them to be overexpressed. Having α -Catenin mutant alleles at the endogenous locus ensures that the expression of the mutant proteins is under normal transcriptional control. A missense mutation was identified in α -Cat¹³, producing a substitution of a methionine residue for the conserved valine at position 851 and thus located in the VH3 actin-binding domain of α -Catenin (Fig. 1C). The other three alleles are nonsense mutations that generate a premature stop codon at residues Q459, Q668 and Q700. The latter two (α -Cat²⁰⁴⁹ and α -Cat¹⁸⁸³, respectively) completely delete the actin-binding domain. α -Cat⁴²¹ deletes the actin-binding domain and part of the VH2 domain, leaving the VBS unaffected (Fig. 1B). Here, we focused on the analysis of the α -Cat¹³, α -Cat²⁰⁴⁹ and α -Cat⁴²¹ alleles.

It has been shown that the VH1 domain is the most important for α -Catenin localisation at the cell membrane (Desai et al., 2013). This suggested that the alleles generated in this work would produce mutant proteins that are able to localise at the cell membrane. Given that visualisation of the localisation of the mutant protein in zygotic mutant embryos is not possible due to the maternal contribution, we assessed the subcellular localisation of the mutant proteins in mitotic recombination clones in wing imaginal discs (Fig. 1D). We observed that the three mutant proteins localised at the membrane in the epithelia of wing imaginal discs, which suggests that they could

interfere with the link between the actomyosin cytoskeleton and the cell membrane.

Although we could not identify the localisation of mutant α -Catenin proteins in the embryos, we analysed whether the levels of full-length α -Catenin were affected in dorsal closure zygotic mutant embryos for our mutants α -Cat¹³, α -Cat⁴²¹ and α -Cat²⁰⁴⁹, as well as for α -Cat¹, a deficiency removing the first exon of α -Cat that includes the translation start site, and therefore is a protein null allele (Sarpal et al., 2012). Immunoblot analysis of stage 13 zygotic mutant embryos (Fig. 1E–G) shows that the levels of the full-length protein (maternal and zygotic) are substantially decreased in extracts from α -Cat²⁰⁴⁹ and α -Cat⁴²¹ homozygous mutant embryos, significantly more than in embryos mutant for α -Cat¹. These results suggest that in α -Cat²⁰⁴⁹ and α -Cat⁴²¹ mutant embryos, there is a destabilisation of the maternal wild-type protein that thus might aggravate the phenotype of an α -Cat-null homozygote. The presence and stability of mutant proteins is difficult to assess: α -Cat¹³ will have the same size as wild-type α -Cat; bands at the predicted truncated size for α -Cat²⁰⁴⁹ were also present in the wild-type, α -Cat¹ and α -Cat¹³ lanes. Although both the α -Cat⁴²¹ and α -Cat²⁰⁴⁹ mutations would render their respective mRNAs sensitive to the nonsense-mediated decay pathway-mediated degradation, this would be expected to lead to null phenotypic conditions (Frischmeyer and Dietz, 1999). Our results below show that this is not the case, which together with the results from the clonal analysis showing that the mutant proteins localise to the cell membrane, lead us to assume that biologically relevant amounts of truncated α -Cat species are present in α -Cat⁴²¹ and α -Cat²⁰⁴⁹ mutant embryos at the dorsal closure stage, but are, however undetectable by western blotting.

We thus hypothesised that these different mutant alleles could help us understand the function of α -Catenin during tissue morphogenesis. The cuticle laid by these embryos develops anterior defects indicative of a failure in head involution (Fig. 1H–N), as has been previously shown for α -Cat¹ (Sarpal et al., 2012). However, we noted that a significant percentage of these embryos also exhibit holes in which the posterior limit of the hole is aligned with the first abdominal segment (Fig. 1J). A small percentage of embryos also developed a complete dorsal open cuticle or dorsal holes (Fig. 1K,L). These phenotypes are indicative of dorsal closure defects and suggest that in α -Cat mutants, both head involution and dorsal closure are compromised. Dorsal closure and head involution are two tightly linked morphogenetic processes involving some of the same tissues and relying on identical genetic pathways (VanHook and Letsou, 2008), and thus it is not uncommon that both processes are affected.

Cellular forces and adhesion during dorsal closure are disrupted in α -Catenin mutants

To better understand why the cuticle defects arise in α -Cat mutant embryos, we took time-lapse movies of homozygous mutant embryos for the different α -Cat alleles carrying an endogenously tagged DE-Cadherin:GFP to visualise cell contours (Fig. 2A; Movies 1, 2). These embryos are able to progress until mid-embryogenesis and to start dorsal closure normally due to the maternal contribution of α -Catenin. However, in most of the embryos defects start appearing during dorsal closure due to the anterior canthus not forming properly: the dorsal ridge primordia, two contra-lateral epithelial structures that form where the dorsal epidermis abuts the head segments, do not elongate, nor move towards the dorsal midline nor fuse to create the dorsal ridge (Fig. 2Aii,ii'). As a consequence, there is no anterior migration of the dorsal ridge and the head segments are left on the outside instead

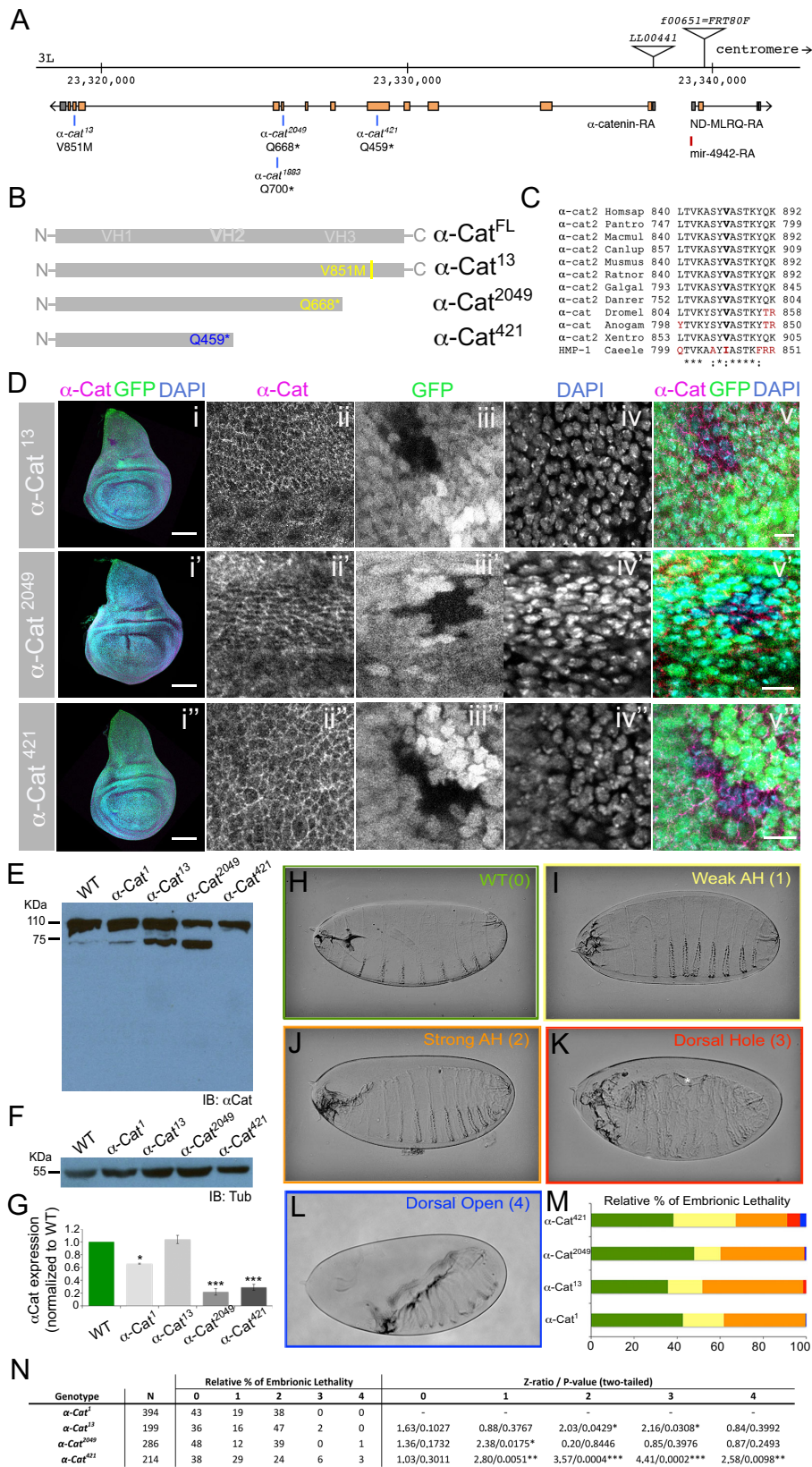


Fig. 1. Characterisation of alpha-Cat alleles.

(A) Schematic representation of the alpha-Cat genomic region of the chromosome used for the mutagenesis. Note that only one transcript is represented for each of the three loci of the region. (B) Schematic representation of alpha-Catenin mutant proteins. (C) Sequence alignment of the C-terminal region of alpha-Catenin. (D) Homozygote mutant clones for the different alpha-Cat alleles in wing imaginal discs. (i–i’) Low-magnification view of wing imaginal discs with the location of the clone indicated. (ii–ii’) Staining for alpha-Catenin. (iii–iii’) The clone, visualised by the lack of GFP, is indicated with a dotted line. (iv–iv’) DAPI signal to label nuclei. (v–v’) Merge. (E, F) Immunoblot of alpha-Catenin in the indicated alpha-Cat stage 13 mutant embryos. WT, wild-type. (G) Quantification of alpha-Catenin signal from four independent experiments. Data show the mean ± s.e.m. *P ≤ 0.05; ***P ≤ 0.001 (unpaired t-test comparison). (H–L) Cuticles of wild-type (H) and different categories of alpha-Cat mutant (I–L) embryos. (M) Quantification of the cuticle defects for each alpha-Cat allele. (N) Statistical differences in the proportion of each phenotypic category between our mutant alleles and the null allele, determined using a two-tailed Z-test (see Materials and Methods). Scale bars: 100 μm (Di–i’), 10 μm (Dii–v’).

of moving inside the dorsal anterior epidermis (Fig. 2Aii,iii’). As dorsal closure progresses, the anterior epidermis and the amnioserosa tear apart. The dorsal-most epidermal cells detach from the amnioserosa in a region spanning the anterior half of the

amnioserosa in several embryos (Fig. 2Aiv,iv’). Meanwhile, the posterior canthus forms and progresses towards the centre of the dorsal midline but tears at the anterior side prevent completion of dorsal closure.

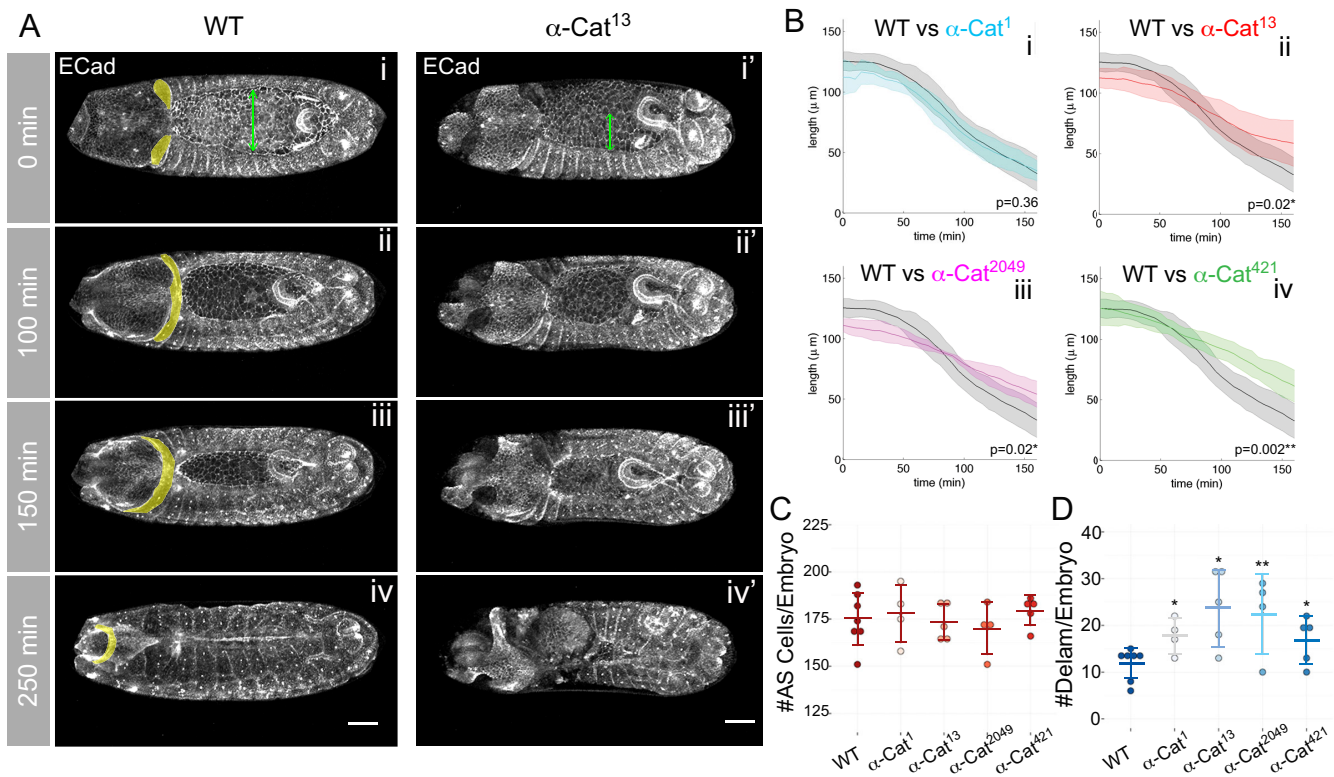


Fig. 2. Live imaging of α -Cat mutant embryos. (A) Still images of example DE-Cadherin:GFP (wild-type, WT; i–iv) and DE-Cadherin:GFP; α -Cat¹³ (i–iv') embryos at the indicated times (similar defects were observed for the other alleles). The dorsal ridge is indicated in yellow and a hole is indicated with a purple dotted line. The width of the amnioserosa is indicated with a green line (i). The green dotted line indicates the length of the amnioserosa (i') and was used as a reference to calculate the half-width of the amnioserosa when one leading edge was out of the plane of view. (B) Quantification of the width of the amnioserosa at its symmetry axis in seven wild-type versus five α -Cat¹ (i), five α -Cat¹³ (ii), four α -Cat²⁰⁴⁹ (iii) and five α -Cat⁴²¹ (iv) mutant embryos. The curve corresponding to the wild-type is always shown in black. Linear regression analysis was performed to get the velocity of dorsal closure progression from 50 min onwards each mutant allele was compared with the wild-type using unpaired *t*-test comparison. *P*-values are indicated in each graph. In these plots, the shaded area corresponds to regions of significant differences applying a linear-mixed effect model (see Materials and Methods). (C) The number of amnioserosa cells at time 0 of dorsal closure and (D) number of cell delamination events in wild-type and α -Catenin mutant embryos. Each dot shows data per embryo. The mean (thick line) and standard deviation (thin lines) are indicated; the mean per genotype was compared to the wild-type using an unpaired *t*-test comparison. **P* ≤ 0.05; ***P* ≤ 0.01. Scale bars: 50 μ m.

To analyse the evolution of dorsal closure quantitatively, we measured the velocity (v) of progression of the leading edge by measuring the width of the amnioserosa at its symmetry axis (Fig. 2A). This provides a quantitative way to assess whether the forces contributing to dorsal closure are affected (Hutson et al., 2009). We observed that in all the alleles analysed there was a decrease in v (Fig. 2Bii,iv) except for α -Cat¹ (Fig. 2Bi), indicating that the point mutations lead to distinct phenotypes. Given that some of the embryos analysed have tears at the anterior canthus as described above, we asked whether the reduction in v resulted largely from the anterior tears. It was possible to test for this in α -Cat¹ and α -Cat⁴²¹ mutant embryos, as not all of the individuals analysed showed anterior tears. Interestingly, we observed that the presence of a hole did not affect v in α -Cat¹ mutant embryos (Fig. S2Ai,ii). However, even in the absence of anterior tears, there was a reduction in v in α -Cat⁴²¹ mutant embryos (Fig. S2Aiii,iv), suggesting that cellular forces contributing specifically to dorsal closure are defective.

One of the processes contributing to dorsal closure is the apoptosis-mediated extrusion from the plane of the amnioserosa epithelium of ~10% of cells (Kiehart et al., 2000), through a mechanism involving cytoskeletal rearrangements in the delaminating cell and also in its nearest neighbours (Meghana et al., 2011; Muliylil et al., 2011). It has

been shown that increasing the number of cell delamination events hastens closure (Toyama et al., 2008). Thus, we asked whether the decrease in closure velocity could be due to a decrease in cell delamination events. We observed that, whereas the total number of amnioserosa cells at the onset of tissue contraction is similar to the wild-type, the number of cell delamination events increased in α -Cat mutant embryos (Fig. 2C,D), but not the location or timing of these events (data not shown). Thus, these results show that changes in the delamination rate are not responsible for the decrease in closure velocity.

These observations suggest that a variety of defects underlie the embryonic phenotype of α -Cat mutant embryos. Time-lapse movies showed that the anterior dorsal ridge is the most affected tissue, disrupting both head involution and dorsal closure. The actin purse string was also affected, as shown by a decrease in actin accumulation (Fig. S2B). Finally, the decrease in closure velocity, which cannot be attributed to the anterior holes or to a decrease in cell extrusions, suggests that the contraction of the amnioserosa might be affected. We are particularly interested in exploring the contribution of α -Catenin to the emergence of the contractile force of the amnioserosa, to understand how actomyosin contractility and adhesion are integrated to give rise to cell and tissue changes in shape.

Loss of α -Catenin slows down the oscillatory and contractile behaviour of amnioserosa cells

To investigate the role of α -Catenin in the contraction of the amnioserosa, we quantitatively analysed the oscillatory and contractile behaviour of amnioserosa cells during the whole process of dorsal closure (Fig. 3; Movie 3). We automatically

tracked amnioserosa cells from four or five embryos for each α -Cat allele and measured the frequency and amplitude of apical cell shape oscillations as previously described (Blanchard et al., 2010). We have previously found that the cycle length and amplitude of apical cell area oscillations shows a temporal pattern over dorsal closure. During the early stages of dorsal closure, amnioserosa

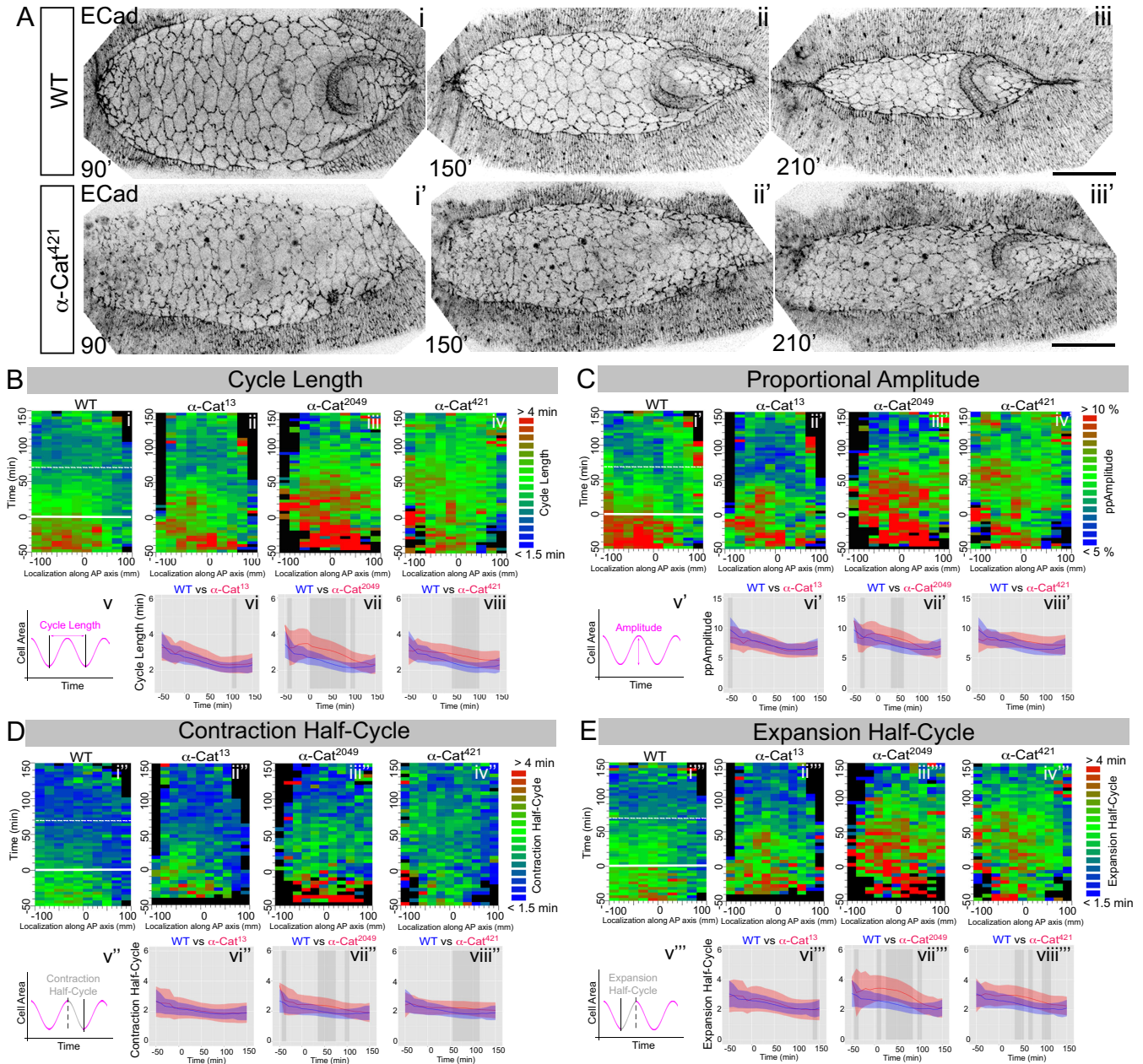


Fig. 3. Apical cell area oscillations in amnioserosa cells of α -Cat mutant embryos. (A) Still images from a time-lapse movie of example DE-Cadherin:GFP (WT; i–iii) and α -Cat⁴²¹ (i'–iii') embryos at 90 min, 150 min and 210 min of dorsal closure. Similar dynamics to α -Cat⁴²¹ was observed for the other alleles. (B–E) Analysis of cell area fluctuations in data pooled from seven wild-type (i–i'''), four α -Cat¹³ (ii–ii'''), four α -Cat²⁰⁴⁹ (iii–iii''') and five α -Cat⁴²¹ (iv–iv''') embryos. (B) Average cycle length of amnioserosa cells as a function of their location along the anterior–posterior axis over time. Anterior is to the left in all similar panels. Cartoon of cycle length (v). Statistical comparison of the cycle length of apical cell area oscillations between the wild-type and the different α -Cat alleles (vi–viii). (C) Average oscillation amplitude as a function of the anterior–posterior location over time. Note that the amplitude of oscillations is a proportional measure expressed as the percentage of the apical cell area. Cartoon showing amplitude (v'). Statistical comparison of the amplitude of apical cell area oscillations between the wild-type and the different α -Catenin alleles (vi–viii). (D) Average contraction half-cycle duration as a function of AP location over time. Cartoon of contraction half-cycle (v''). Statistical comparison of the contraction half-cycle duration between the wild-type and the different α -Cat alleles (vi–viii). (E) Average expansion half-cycle duration as a function of their anterior–posterior location over time. Cartoon of expansion half-cycle (v'''). Statistical comparison of the expansion half-cycle duration between the wild-type and the different α -Cat alleles (vi–viii). In these plots, the shaded area corresponds to regions of significant differences applying a linear-mixed effect model (see Materials and Methods). Continuous and dotted white lines in wild-type panels (B–E) indicate the transition between different oscillatory modes. Scale bars: 50 μ m.

apical cell area fluctuated with long cycle lengths and high amplitude. The onset of whole-tissue contraction coincided with a decrease in both the cycle length and the amplitude of cell oscillations. At 60 min into this phase, zippering from the canthi engaged, and cells entered a fast mode of oscillations with low amplitude and short cycle length.

In α -Cat¹³ mutant embryos, the spatiotemporal pattern of the cycle length of apical cell area oscillations was almost identical to the wild-type (Fig. 3B). The amplitude of cell oscillations was only mildly affected in α -Cat²⁰⁴⁹ and not at all in α -Cat⁴²¹ embryos (Fig. 3C). By contrast, there was a clear increase in the period of oscillations in α -Cat²⁰⁴⁹ mutant embryos for almost 2 h of development. α -Cat⁴²¹ embryos displayed a similar, although milder increase in period, mostly at later stages (Fig. 3B). Our previous results have shown that an important signature of the pulsatile contractile behaviour is the ratio of the duration of the expansion half-cycle to the contraction half-cycle, with lower ratios being consistent with a more-contracted state (Blanchard et al., 2010). Thus, we analysed whether the duration of the half-cycles was differentially increased in these mutant embryos. We observed an increase in both the contraction and the expansion half-cycle lengths in α -Cat²⁰⁴⁹ and α -Cat⁴²¹ mutants, with the expansion half-cycle being more significant, and over a longer developmental period (Fig. 3D,E). This is also evident in the ratio of the duration of the expansion half-cycle to the contraction half-cycle, which is greater in α -Cat²⁰⁴⁹ and α -Cat⁴²¹ but not in α -Cat¹³ mutant embryos (Fig. S3A). Thus, these results suggest that amnioserosa cells are not contracting properly in α -Cat²⁰⁴⁹ and α -Cat⁴²¹ mutant embryos. In accordance with this, the rate of apical cell contraction is lower in these embryos (Fig. S3B). Interestingly, we found that amnioserosa cells from α -Cat⁴²¹ and α -Cat²⁰⁴⁹ mutant embryos develop a corrugated appearance (Fig. 3Aii', compare with Aii), which indicates that the apical cell perimeter is not able to shrink properly.

We measured the ratio of apical cell perimeter to apical cell radius and observed a significant increase in this ratio in the later stages of dorsal closure (Fig. S3C). Taken together, our results show that the apical contraction of these cells is defective.

α -Catenin regulates the dynamics of actomyosin foci

Apical cell oscillations result from Myosin-driven oscillatory contractions of a medial actin network spanning the apical medial region of amnioserosa cells (Blanchard et al., 2010; David et al., 2010). Myosin and actin colocalise tightly at the medioapical cortex of amnioserosa cells forming transient accumulations or foci, and both Myosin and F-actin reporters can be used to follow their dynamics (Blanchard et al., 2010; David et al., 2010). To elucidate whether the slower oscillatory dynamics in α -Cat mutants result from perturbed actomyosin activity, we took time-lapse movies of amnioserosa cells carrying the F-actin reporter sGMCA (Movies 4, 5). Then we measured the duration and time interval of F-actin foci over a 15-min time window, during the slow phase of dorsal closure (Fig. 4A,B) when oscillation defects are more important.

The mean duration of the actin cycle increases in amnioserosa cells from α -Cat²⁰⁴⁹ and α -Cat⁴²¹ mutant embryos but not in α -Cat¹³ embryos (Fig. 4C), correlating with an increased period of cell oscillations in the former but not in the latter mutant backgrounds. Interestingly, the time interval between consecutive actin foci increased for the three alleles, but significantly more in α -Cat⁴²¹ and α -Cat²⁰⁴⁹ mutant embryos (Fig. 4D). This suggests that the increase in the expansion half-cycle length in these embryos could be a direct consequence of the increase in the time interval between consecutive foci. In contrast, the duration of actin foci decreased in α -Cat¹³ and α -Cat⁴²¹, but not in α -Cat²⁰⁴⁹ embryos (Fig. 4E). Thus, the observed dynamics of actin foci shows a correlation with the oscillatory behaviour of amnioserosa cells; however, in α -Cat²⁰⁴⁹ and α -Cat⁴²¹ mutant embryos, the increase in

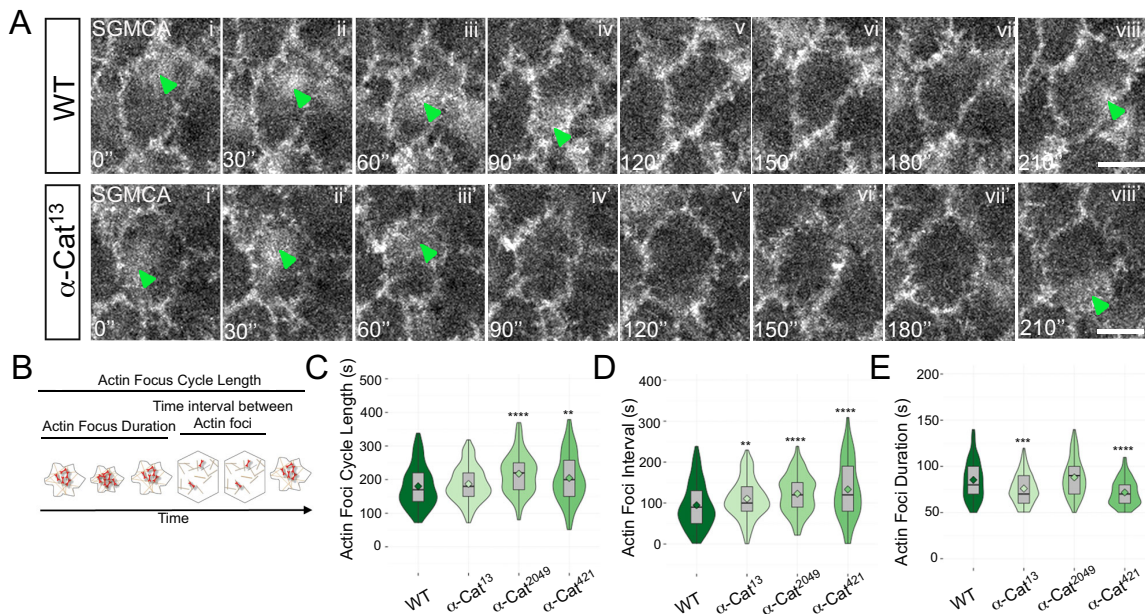


Fig. 4. Dynamics of actin foci in amnioserosa cells in α -Cat mutant embryos. (A) Still images of example sGMCA (wild-type WT; i–vi) and sGMCA; α -Cat¹³ (i'–vi') embryos, with actin foci indicated with arrowheads in green. (B) Cartoon depicting the cycle length, duration and time interval between the appearances of actomyosin foci. (C–E) Violin plots displaying the probability density of the data at different values for the cycle length (C), time interval (D) and duration (E) of actin foci from wild-type (188 foci from six embryos), α -Cat¹³ (158 foci from five embryos), α -Cat²⁰⁴⁹ (112 foci from four embryos) and α -Cat⁴²¹ (86 foci from four embryos) embryos. See also Table S1. The mean (diamond) and median (line) are indicated in the box plot inside each violin plot. We performed a Mann–Whitney test to assess if the means for each mutant were significantly different to control: ** $P \leq 0.01$; *** $P \leq 0.001$; **** $P \leq 0.0001$. Scale bars: 10 μ m.

the time interval between consecutive foci gives rise to an increase in the cycle length of cell oscillations, this is not the case in α -Cat^{L3} embryos, where the low increase in the time interval between consecutive foci together with the decrease in the duration of actin foci cancel out and give rise to a whole actin cycle length indistinguishable from the wild type.

To confirm that this change in actin dynamics is a consequence of a defective link between the cytoskeleton and adherens junctions, we also analysed actin dynamics in DE-Cadherin mutant embryos, which provide a situation where α -Catenin levels are further reduced. The *shg*^{g317} mutant allele codes for a truncated DE-Cadherin protein lacking the Armadillo-binding domain (Gorfinkiel and Martínez Arias, 2007), thus preventing the

interaction of DE-Cadherin with α -Catenin. This allele has a stronger phenotype than the null allele, probably through a dominant-negative effect on the maternal protein (Gorfinkiel and Martínez Arias, 2007; Tepass et al., 1996). Time-lapse imaging of *shg*^{g317} mutant embryos carrying the sGMCA reporter (Movie 6) showed that amnioserosa cells form actin foci but these showed a significantly shorter duration, as well as longer time intervals between consecutive foci, than in wild-type embryos (Fig. 5A–D; Table S1).

Overall, our results suggest that α -Catenin has a role in stabilising actomyosin foci and in promoting the formation of new foci. Interestingly, α -Catenin also regulates medial actomyosin dynamics and polarity in germband cells (Rauzi et al., 2010). The particular

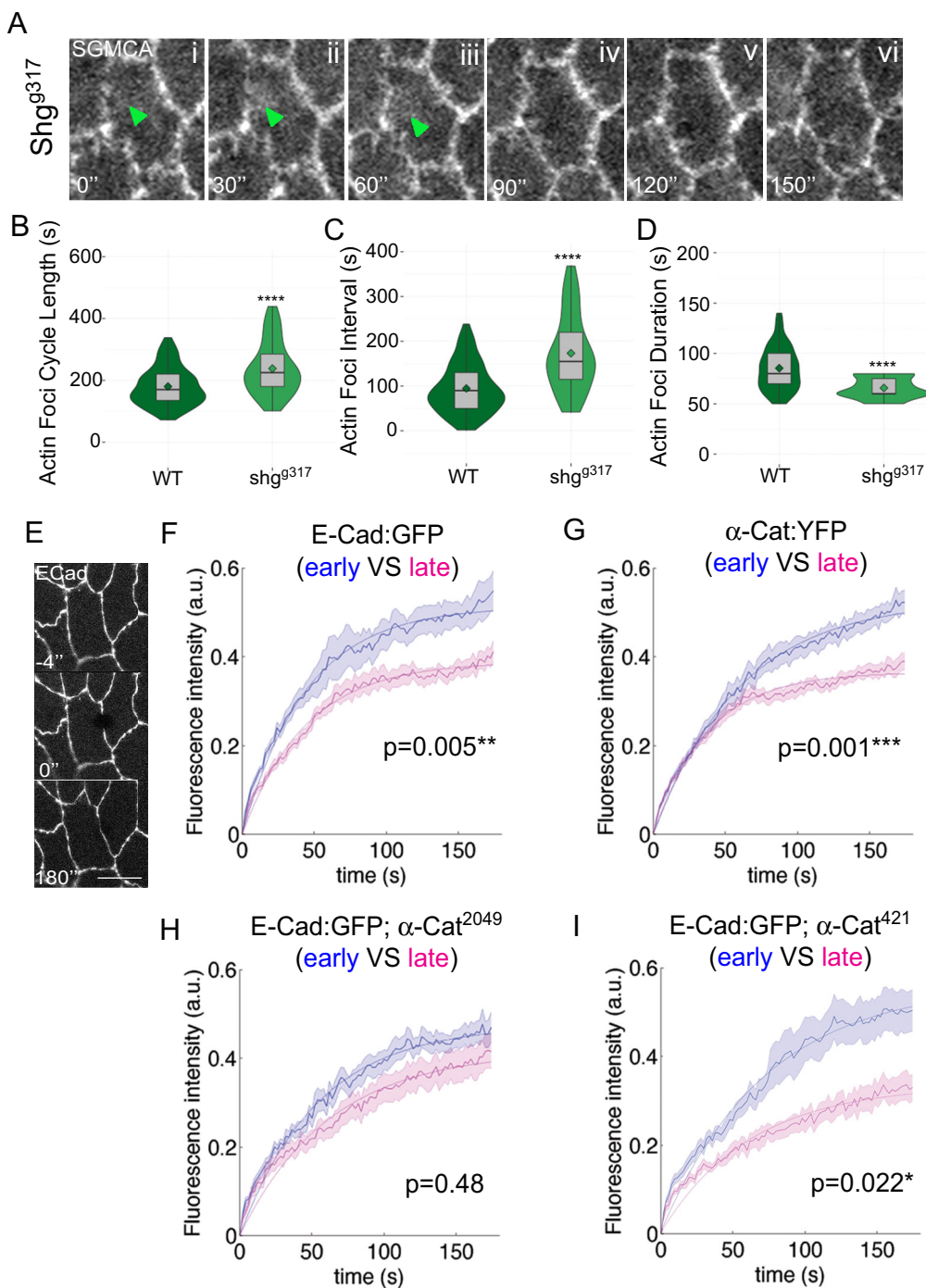


Fig. 5. Dynamics of actin foci in amnioserosa cells in *shg* mutant embryos. (A) Still images of an example sGMCA; *shg*^{g317} embryo (i–vi), with actin foci indicated with arrowheads in green. (B–D) Violin plots displaying the probability density of the data at different values for the cycle length (B), the time interval (C) and the duration (D) of actin foci from *shg*^{g317} mutants (40 foci from four embryos). See also Table S1. (E–I) FRAP analysis (the yellow circle in E shows the bleached area) of DE-Cadherin:GFP (11 cells from seven early dorsal closure and 13 cells from seven late dorsal closure embryos) (F) and α -Catenin:YFP (12 cells from five early dorsal closure and 18 cells from eight late dorsal closure embryos) (G) in the amnioserosa of embryos during early and late stages of dorsal closure. Note the reduction on the mobile fraction of both proteins as dorsal closure progresses. In α -Cat²⁰⁴⁹ mutant embryos (12 cells from eight early dorsal closure and 14 cells from seven late dorsal closure embryos), there is no decrease in the mobile fraction of DE-Cadherin:GFP (H). In α -Cat⁴²¹ mutant embryos (17 cells from six early dorsal closure and 10 cells from five late dorsal closure embryos), there is a reduction in the mobile fraction of DE-Cadherin:GFP (I). These plots represent the mean of all the experiments for each condition and the shaded area represents the standard error. Comparisons between early and late mobile fractions show the following statistical significance from unpaired *t*-test comparison: **P*≤0.05; ***P*≤0.01; ****P*≤0.001. Scale bars: 10 μ m.

dynamics of actin foci observed in the alleles analysed here suggest that the interaction of α -Catenin with actin and other actin-binding proteins might be differentially affected in each specific allele.

E-Cadherin dynamics at cell-cell junctions in α -Catenin mutants

It is known that α -Catenin is required for adherens junction assembly, function and dynamics (Cavey et al., 2008; Desai et al., 2013; Imamura et al., 1999; Pacquelet and Rorth, 2005; Sarpal et al., 2012; Yonemura et al., 2010). Moreover, it has been shown that the actin-binding domain of α -Catenin, and hence the interaction of α -Catenin with the actin cytoskeleton, promotes the localisation of DE-Cadherin and Armadillo at the apical cell membranes (Desai et al., 2013). We thus analysed whether DE-Cadherin levels were also affected in α -Cat mutant embryos. We could not detect significant changes in DE-Cadherin levels in α -Cat zygotic mutant embryos, but did detect changes in DE-Cadherin turnover. Fluorescence recovery after photobleaching (FRAP) experiments on endogenously-tagged DE-Cadherin:GFP embryos showed that there was a significant decrease in the mobile fraction of DE-Cadherin as dorsal closure progresses, suggesting that DE-Cadherin is stabilised at cell membranes during late stages of the process (Fig. 5E,F). Similarly, FRAP experiments on an α -Catenin:YFP protein trap that is homozygous viable and localises normally to the cell membrane, also showed a decrease in the mobile fraction of α -Catenin as dorsal closure progresses (Fig. 5G). However, in α -Cat²⁰⁴⁹ mutant embryos the decrease in DE-Cadherin mobile fraction as dorsal closure progresses did not occur (Fig. 5H). Surprisingly, in α -Cat⁴²¹ mutant embryos, the stabilisation of DE-Cadherin with developmental time was recovered (Fig. 5I). These results show that adhesion dynamics is different in α -Cat²⁰⁴⁹ and α -Cat⁴²¹ mutant backgrounds. Interestingly, truncated forms of α -Catenin that bind constitutively to Vinculin strongly stabilise adherens junctions dynamics (Chen et al., 2015; Yonemura et al., 2010). Given that the α -Cat⁴²¹ allele removes not only the actin-binding domain but also part of the VH2 domain, our results raise the possibility that in α -Cat⁴²¹ embryos, constitutive binding of α -Catenin to Vinculin rescues DE-Cadherin dynamics.

Interaction between Vinculin and α -Catenin

In mammalian cells, Myosin-II-generated tension induces a conformational change in α -Catenin uncovering a VBS. Vinculin is then recruited to adherens junctions and becomes associated with more actin filaments thus reinforcing cell–cell adhesion (Kim et al., 2015; le Duc et al., 2010; Yao et al., 2014; Yonemura et al., 2010). Thus, we decided to investigate whether Vinculin and α -Catenin also interacted during *Drosophila* embryogenesis. A complete deletion of the Vinculin-coding sequence ($\Delta Vinc$) is viable and does not cause any visible phenotype (Klapholz et al., 2015). However, $\Delta Vinc$ aggravated the cuticular phenotype of α -Cat mutant embryos in an allele-dependent manner, with a decreasing strength series of α -Cat²⁰⁴⁹> α -Cat¹³> α -Cat¹> α -Cat⁴²¹, with the latter showing only a very weak genetic interaction (Fig. 6A,C). These results indicate that α -Cat genetically interacts with *Vinculin*. They further show that, although the absence of Vinculin does not affect the viability of *Drosophila* embryos and adults, in some α -Catenin mutant backgrounds its activity is able to partially compensate for α -Catenin function. Curiously, the α -Cat⁴²¹ allele showed the weakest genetic interaction showing that, in this allele, Vinculin is not able to partially restore α -Catenin function.

A possible explanation for these results is that the α -Catenin²⁰⁴⁹ and α -Catenin¹³ mutant proteins expose the VBS and bind to

Vinculin, which, by its binding to the actin cytoskeleton, restores α -Catenin function. This would not happen in the α -Catenin⁴²¹ mutant protein, given that the absence of Vinculin does not aggravate the phenotype of this allele. However, this is in sharp contrast with what is known about the molecular interaction between α -Catenin and Vinculin. According to the current paradigm, the α -Cat²⁰⁴⁹ protein, which lacks the actin-binding domain (Fig. 1B), would not be stretched to expose the VBS and therefore would not interact molecularly with Vinculin. By contrast, the α -Cat⁴²¹ protein, whose truncation removes the putative auto-inhibitory domain (Fig. 1B), would have an exposed VBS and thus would interact with Vinculin in a constitutive manner.

To better understand these results, we tested the ability of the α -Cat alleles to interact with the actomyosin cytoskeleton, by ectopically expressing a phosphomimetic form of the Myosin Regulatory Light Chain (also known as Spaghetti squash, Sqh), Sqh^{DD}, in the amnioserosa of α -Cat mutant embryos. We hypothesised that increasing actomyosin contractility in the amnioserosa of embryos in which E-Cadherin-mediated adhesion is compromised would lead to stronger and more frequent tears if α -Catenin were indeed able to transmit contractile forces to the cell membranes. We observed that the ectopic expression of Sqh^{DD} in the amnioserosa aggravated the cuticular defects of α -Cat¹ and α -Cat¹³ embryos, but did not have an effect on the cuticular phenotypes of α -Cat²⁰⁴⁹ and α -Cat⁴²¹ embryos (Fig. 6B,C). These results confirm that neither α -Cat²⁰⁴⁹ nor α -Cat⁴²¹ is able to interact properly with the actomyosin cytoskeleton.

Thus, an alternative explanation that reconciles our results with what is known about the α -Catenin–Vinculin interaction is that in all but the α -Cat⁴²¹ allele, the presence of Vinculin partially rescues the function of α -Catenin, but this rescue is not dependent on the ability of these proteins to interact at the molecular level. Interestingly, an α -Catenin-independent binding of Vinculin to E-Cadherin has been observed in cancer cells devoid of α -Catenin (Hazan et al., 1997). In contrast, in the α -Cat⁴²¹ allele, this function of Vinculin would be prevented because most Vinculin would be bound to α -Catenin in a constitutive manner.

These results led us to analyse Vinculin localisation in the amnioserosa of embryos undergoing dorsal closure. Recently, a genomic construct containing Vinculin:GFP has been generated, providing a reporter with physiological expression levels (Klapholz et al., 2015). Vinculin:GFP can be seen localising at the apical side of epidermal cells, but in amnioserosa cells from early dorsal closure embryos, fluorescence levels were very low. We observed a small but consistent increase of Vinculin:GFP at the level of the cell membranes in late dorsal closure embryos compared to at early stages of the process (Fig. 6D), when cells contract faster. We further analysed whether this Vinculin localisation was dependent on tension. We observed an increase of Vinculin levels in early dorsal closure embryos when Myosin activity is elevated in the amnioserosa through the ectopic expression of a constitutive active form of Myosin Light Chain Kinase (Fig. 6E). Similar results were observed with a UAS-Vinculin:YFP reporter expressed in the amnioserosa: Vinculin localisation at the apical membrane of amnioserosa cells increased as dorsal closure progresses (Fig. S4A), and this localisation increases and decreases when constitutive active forms of Myosin Light Chain Kinase and Myosin phosphatase, respectively, are ectopically expressed (Fig. S4B,C).

Finally, we analysed the localisation of the Vinculin reporter in α -Cat²⁰⁴⁹ and α -Cat⁴²¹ mutant backgrounds. We found that in both mutant backgrounds, Vinculin localised to apical cell membranes (Fig. 6F) and its levels were increased in later embryos compared to

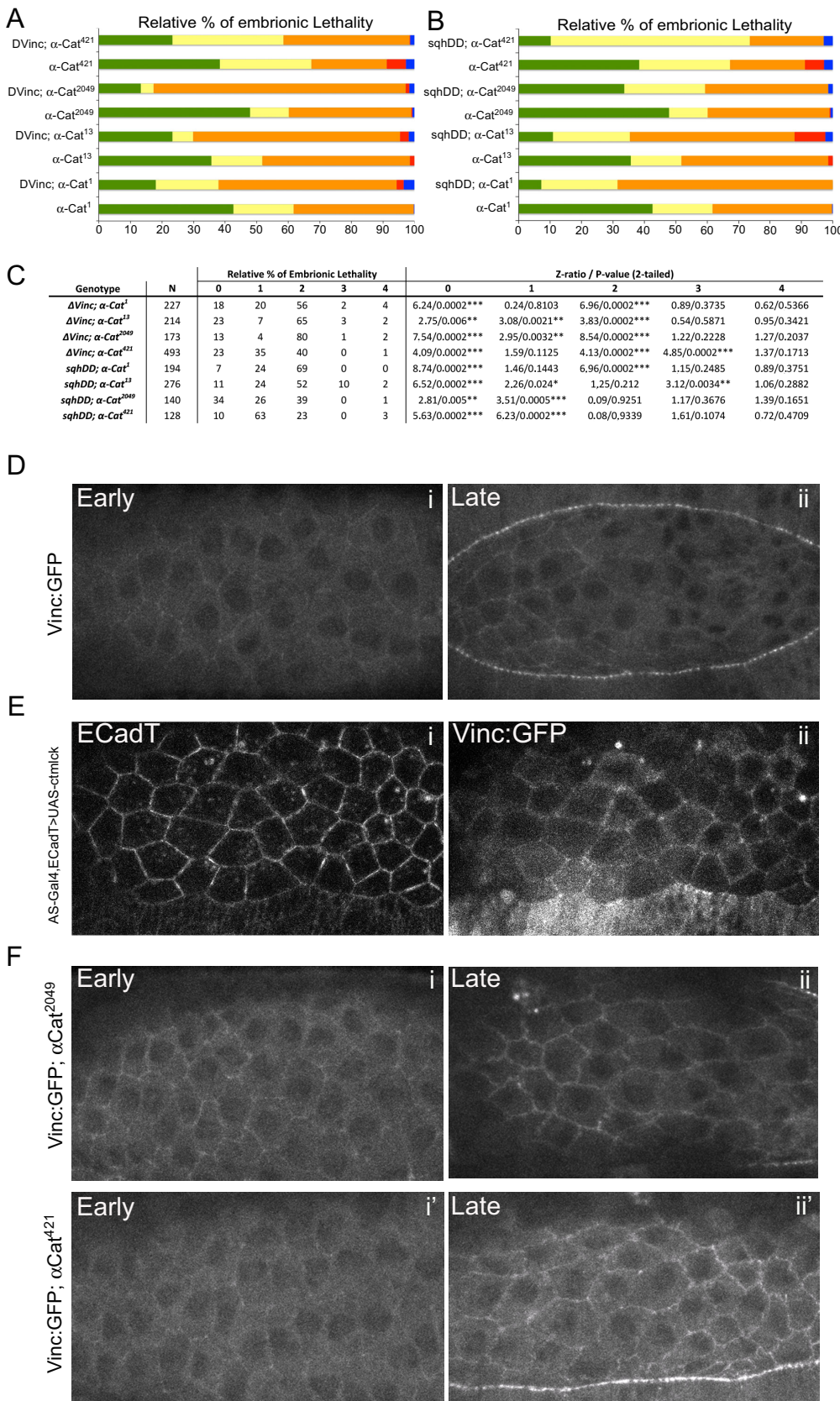


Fig. 6. Interaction between α -Cat and Vinculin and the actomyosin cytoskeleton. (A) Quantification of the cuticle defects from embryos double homozygous for *Vinculin* and the different α -Cat alleles. (B) Quantification of the cuticle defects from α -Cat mutant embryos in which *Sqh^{DD}* is ectopically expressed in the amnioserosa. (C) Statistical differences in the proportion of each phenotypic category between each mutant allele and the null allele. * $P \leq 0.05$; ** $P \leq 0.01$; *** $P \leq 0.001$, determined using a two-tailed Z-test (see Materials and Methods). (D) Localisation of Vinculin:GFP in amnioserosa cells from early and late dorsal closure stages (i,ii). (E) Localisation of E-Cadherin:mTomato (i) and Vinculin:GFP (ii) in early dorsal closure embryos in which a constitutive active form of MLCK has been ectopically expressed in the amnioserosa. (F) Localisation of Vinculin:GFP in amnioserosa cells from early (i,i') and late (ii,ii') dorsal closure stages in α -Cat²⁰⁴⁹ (i,ii) and α -Cat^{Δ21} (i',ii') embryos. Scale bars: 25 μ m.

the wild-type. We hypothesise that in α -Cat²⁰⁴⁹ embryos, Vinculin localises at cell–cell junctions independently of α -Catenin, whereas in α -Cat^{Δ21} embryos, Vinculin localises at cell–cell junctions through direct binding with α -Catenin.

Taken together, our results suggest that there is a tension-dependent recruitment of Vinculin to the apical membranes of amnioserosa cells. Moreover, the observed interactions between α -Catenin and Vinculin suggest both α -Catenin-dependent and

α -Catenin-independent roles for Vinculin during *Drosophila* embryogenesis.

DISCUSSION

How adhesion and actomyosin contractility are integrated at junctions is a fundamental question in morphogenesis. To tackle this, we have analysed the role of α -Catenin, a key protein linking adherens junctions and the actin cytoskeleton, in the context of *Drosophila* embryogenesis and in particular during dorsal closure. We find that α -Catenin regulates pulsatile actomyosin dynamics in apically contracting cells by stabilising and promoting actomyosin contractions. α -Catenin also stabilises DE-Cadherin at the cell membrane, suggesting that medioapical actomyosin contractility regulates junction stability. Furthermore, our results reveal an interaction between α -Catenin and Vinculin that could be important for DE-Cadherin stabilisation.

Our live imaging of mutant embryos shows a strong requirement for α -Catenin in the migration of the dorsal ridge primordia towards the dorsal midline, preventing the formation of the dorsal ridge and thus affecting both dorsal closure and head involution. These results reveal that the dorsal ridge is particularly sensitive to the levels of α -Catenin and suggest it is a key region that could mechanically coordinate both processes. Although it is clear that some of the defects we observe during dorsal closure are a consequence of the defective dorsal ridge morphogenesis, our analysis shows that other cellular processes more specific to dorsal closure are affected. In particular, we observe that the actin cable is disorganised and that the pulsatile apical contraction of the amnioserosa is abnormal.

The defects observed at the level of amnioserosa apical cell oscillations could be a consequence of a defective actin cable, which would be acting as a ratchet and thus progressively restricting the expansion of apical cell area (Solon et al., 2009). However, several lines of evidence suggest that a ratchet mechanism stabilising the contracted state of amnioserosa cells is acting at the level of individual cells (Blanchard et al., 2010; Wang et al., 2012; Wells et al., 2014). In particular, the analysis performed here of actin oscillatory dynamics in α -Cat mutants suggests that the increase in the expansion half-cycle of amnioserosa apical cell oscillations could be due to an increase in the time interval between the appearance of consecutive foci. Thus, our results favour the idea that the Cadherin–Catenin complex has a role in promoting actomyosin oscillatory dynamics. How α -Catenin promotes actomyosin contractility remains to be elucidated, but it is likely to involve both direct and indirect (through other actin-binding proteins) interactions with the actin cytoskeleton. For example, an antagonistic interaction between α -Catenin and the Arp2/3 complex has been observed both in cell systems and in *Drosophila* embryos (Benjamin et al., 2010; Sarpal et al., 2012), raising the possibility that the actin-bundling activity of α -Catenin at adherens junctions, rather than the formation of Arp2/3-dependent networks, could be important for apical contraction.

Interestingly, we find that with the α -Cat²⁰⁴⁹ allele, adhesion dynamics are also defective, suggesting that medioapical actomyosin dynamics promote adherens junction stabilisation. In contrast, with the α -Cat⁴²¹ allele, which would bind constitutively to Vinculin in a context of defective medioapical actomyosin dynamics, DE-Cadherin stabilisation is recovered. This result suggests that the stabilisation of DE-Cadherin could be mediated by the binding of Vinculin to α -Catenin. This is in agreement with what has been observed in cell systems, where forms of α -Catenin that constitutively bind to Vinculin have decreased mobility (Cheng et al., 2015; Yonemura et al., 2010). We further show that, although DE-Cadherin

is stabilised in α -Cat⁴²¹ mutants, possibly due to the Vinculin– α -Catenin interaction, this stabilisation is not able to rescue normal medioapical actin dynamics. Thus, we suggest that direct binding of α -Catenin to actin through its actin-binding domain promotes the formation of medioapical actomyosin foci, whereas indirect binding to actin through Vinculin would promote junction stabilisation. Taken together, our data suggest that α -Catenin domains, through their interactions with other actin-binding proteins and actin, might differentially regulate actin dynamics.

Finally, our results show that there is a tension-dependent recruitment of Vinculin at the membranes of amnioserosa cells, which could be mediated by α -Catenin. Interestingly, it has recently been found, in experiments using a heat-shock inducible Vinculin reporter, that the rate of change of Vinculin levels correlates with junctional tension (Hara et al., 2016). Our results also suggest that Vinculin is able to perform an adhesive function when α -Catenin function is compromised. This could result from an α -Catenin-independent binding of Vinculin to E-Cadherin (Hazan et al., 1997) or from an interaction between Vinculin and other junctional proteins such as ZO-1 (also known as TJP1), which has been shown to recruit Vinculin to VE-cadherin junctions and increase cell–cell tension (Tomavaca et al., 2015). However, given that ZO-1 can also interact with α -Catenin, it remains to be investigated whether the mechanosensitivity of Vinculin is completely dependent on α -Catenin. Thus, it is likely that Vinculin is able to perform different functions depending on its developmental context. Interestingly, different mechanisms for Vinculin binding to Talin in integrin-mediated adhesion have recently been uncovered in different morphogenetic processes, meaning that Talin can sense different force vectors (Klapholz et al., 2015). Given that a role for Talin and integrin-mediated adhesion during dorsal closure has been uncovered (Ellis et al., 2013; Narasimha and Brown, 2004; Reed et al., 2004), it would be interesting to investigate whether Vinculin is also involved in integrin-mediated adhesion at this stage. Our results suggest that a tension-dependent module involving Vinculin is present in amnioserosa cells. An exciting avenue will be to identify the mechanisms and function of such module in the context of morphogenesis.

MATERIALS AND METHODS

Fly stocks and genetics

The stocks used in this work are listed in Table S2.

Mutagenesis

Mutagenesis was performed on a *w*; *PBac*{*WH*}*ND-MLRQ*⁰⁰⁶⁵¹ background, isogenic for the third chromosome. *PBac*{*WH*}*f00651* is inserted at position 23,339,695 of release r6.09 of the *Drosophila melanogaster* genome (estimated cytological band 80E1), ~2 kb proximal to the transcriptional start site of *α-Cat*. It contains a long FRT sequence to allow for the generation of molecularly defined deletions (Thibault et al., 2004), which also makes it apt for mitotic recombination-mediated clonal analysis (see Fig. 1D). This background was selected because the *α-Cat* locus is proximal to both FRT80B and FRT2A. Although the *PBac*{*WH*}*f00651* insertion probably disrupts *ND-MLRQ* function, we found it to be homozygous viable, but with somewhat reduced fertility. For simplicity, we renamed this strain as *w*; *FRT80E1*. We treated 2–3-day-old, pre-starved (8 h) *w*; *FRT80E1* males with ~0.3% ethyl methanesulfonate in 1% sucrose for 24 h, and crossed them to *w*; *MKRS/TM6B* virgin females. Approximately 4000 males from the offspring were crossed individually to *α-Cat*^{L004411}/*TM6B* virgin females. *α-Cat*^{L004411} originates from a lethal *PBac*{*S**AstopDsRed*} insertion (Schuldiner et al., 2008) and is a probable transcriptional null. Offspring was tested for complementation of lethality. These lines were re-tested with a custom deficiency between the FRT-bearing insertions *P*{*RS3*}*CB-6208-3* (Ryder et al., 2004), located at 23,339,498 (r6.09) (our results), and *PBac*{*WH*}*ND-MLRQ*⁰⁵⁹⁶⁶ (Thibault

et al., 2004), located at 22,998,301 (r6.09) (Ryder et al., 2004; and our results). This deficiency uncovers the whole α -Cat locus as well as other genes and has a strong minute phenotype.

Construction of transgenic line

For construction of the UAS-Vinculin:Venus construct, the cDNA was amplified by PCR, cloned into the entry vector pENTR/D-TOPO by directional TOPO cloning (Gateway System, Invitrogen) and introduced by recombination into the destination vector pTWV (pUAS-Venus).

Live imaging

Stage 12–13 *Drosophila* embryos were dechorionated, mounted on coverslips with the dorsal side glued to the glass and covered with Voltalef oil 10S (Attachem). The amnioserosa was imaged at 25–28°C using an inverted LSM 710 Meta laser-scanning microscope with a 40 \times or a 63 \times oil immersion Plan-Fluor objective. For whole amnioserosa imaging, 15 or 16 z-sections 1.5- μ m apart were collected every 30 s. For cytoskeletal dynamics imaging, five or six z-sections 1- μ m apart were collected every 15 s.

FRAP experiments

FRAP was performed using an LSM710 laser-scanning microscope with a 63 \times oil immersion Plan-Apochromat (NA 1.4) objective. A circular region of interest (ROI) ($r=0.52\ \mu\text{m}$) was bleached with a 488-nm laser beam at 100% power. Images were taken before and after bleaching every 2 s for 2 min. A 3.2 \times 3.2 μm reference region was also imaged to take into account photobleaching effects. For FRAP analysis, the normalised fluorescence over time for each individual experiment was fitted to a simple exponential function of the form: $I(t)=A[1-\exp(-bt)]$ using the MATLAB built-in function `nlinfit` and `nlparci` (MathWorks, Natick, MA), where A is the mobile fraction and b is $\ln 2/\tau_{1/2}$, where $\tau_{1/2}$ is the half time of the recovery. Mean parameters were calculated for each genotype. To assess the significance of differences between early and late embryos in each genotype, we applied a two sample t -test (Statistics toolbox of MATLAB).

Image analysis

Four or five embryos for each α -Cat allele were used for the morphometric analysis of amnioserosa cells. Embryos analysed were not selected on the basis of their gross phenotype and are representative of all the embryos that were imaged. (All embryos imaged and analysed had anterior detachments of varying gravity, except in the case of the α -Cat⁴²¹ allele, for which embryos with and without anterior detachments were analysed, but no differences in the parameters analysed were observed between the two classes.) Automated tracking of the amnioserosa cell shapes was performed with custom software written in Interactive Data Language (IDL, Exelis) as described previously (Blanchard et al., 2009, 2010). Cell shape fluctuations were analysed as described previously (Blanchard et al., 2010). Individual embryos were staged according to three parameters, which have been shown to evolve stereotypically throughout the course of dorsal closure (Gorfinkiel et al., 2009): cell area, cell shape anisotropy and mediolateral cell length (Fig. S1). This allowed us to determine their developmental time with an accuracy of 10 min. Inter-genotype aligning was performed by aligning the tissue strain rate, which, in the case of α -Cat mutant embryos, might underestimate possible delays in the onset of net tissue contraction.

Actin foci dynamics was computed manually from time-lapses movies with a 15-s-time interval, which allowed us to follow the assembly and disassembly of each focus in an accurate manner. Central cells of the amnioserosa were chosen to quantify actin dynamics. The times associated with the duration of foci were obtained by counting the number of frames between when an actin focus appeared until its signal was lost. The times associated with the time interval between consecutive foci appearing were obtained by counting the number of frames in which no apicomedial actin signal was detected.

Immunostainings

Embryos were fixed and stained as previously described (Kaltschmidt et al., 2002). Primary antibody was rat monoclonal against α -Catenin (DCAT-1,

1:20, Developmental Studies Hybridoma Bank, University of Iowa, developed by Takeshi Uemura). Alexa-Fluor-555-conjugated anti-rat-IgG (1:500 ThermoFisher) was used as secondary antibody. DAPI (1:200, Merck) was used for imaginal discs stainings. For actin staining, Phalloidin-TRITC (P-1951, 1:500, Sigma) was added to the paraformaldehyde (PFA; 8% solution, EM grade, Electron Microscopy Sciences) and ethanol 80% was used instead of methanol 100%. F-actin fluorescence was quantified using ImageJ.

Immunoblotting

Stage 13 dechorionated embryos were homogenised in SDS sample buffer (62.5 mM Tris-HCl pH 6.8, 2.3% SDS, 10% glycerol, 5% β -mercaptoethanol and 0.005% Bromphenol Blue). Proteins resolved by SDS-PAGE were transferred into nitrocellulose membranes (Amersham). Membranes were blocked in PBS containing 5% milk powder and 0.05% Tween-20 for 1 h at 25°C, incubated overnight with primary antibodies at 4°C and then with a horseradish-peroxidase-conjugated anti-rat-IgG secondary antibody (1:1000, Jackson ImmunoResearch) for 1 h at room temperature. After extensive washes in PBS with 0.05% Tween-20, bands were visualised using the ECL system (Biosciences). The following primary antibodies were used: anti- α -Catenin (rat monoclonal DCAT-1, 1:400, DSHB) and anti- β -tubulin (mouse monoclonal E7, 1:1000; DSHB).

Cuticle preparations

Embryos were collected from 24-h-old eggs and then aged 48 h at 25°C. They were dechorionated in bleach and mounted with the vitelline membrane in acetic acid and Hoyer's (1:1) and the slide was incubated overnight at 65°C.

Statistics

Statistical analysis of embryonic cuticles was done using a two-tailed Z -test, which evaluates the significance of the difference of the z -ratio between two independent proportions. Each proportion was calculated by dividing the number of observations within each phenotypic category by the total number of observations. Each allele was compared to the null allele α -Cat¹. A z -ratio greater than 1.64, 2.33 or 3.09 corresponds to $P<0.05$, <0.01 or <0.001 , respectively. Statistical analysis of actin foci dynamics was performed by considering each focus as an individual event, and then computing the duration and time interval of each focus individually. Pooled data of these variables was then compared between genotypes using a Mann-Whitney U -test given that they did not follow a standard normal distribution, previously tested with a one-sample Kolmogorov-Smirnov test (Statistics ToolBox of MATLAB). Statistical analysis of cell oscillations and other cell parameters was performed by using a mixed-effect model as described previously (Butler et al., 2009; Fischer et al., 2014). We estimated the P -value associated with a fixed effect of differences between genotypes, allowing for random effects contributed by differences between embryos within a given genotype, calculated at each time point. Ribbons were drawn for the whole span of analysis for wild-type embryos and for mutant embryos. The mean trends and ribbon width are calculated from data averaged to reduce noise (a box average of eight bins along the abscissa was used). The widths of ribbons straddling mean trends represent a standard error calculated from the sums of within-experiment variance and between experiments variance. To test where mutant embryos were significantly different ($P<0.05$) from wild-type, mixed-model was applied, with the embryo as the random variable. The regions where $P<0.05$ are depicted with a grey-shaded box.

Acknowledgements

We are very grateful to Guy B. Blanchard for the development of 'oTracks' software and for discussions, and to Alfonso Martinez Arias, in whose laboratory the mutagenesis was performed. We thank Nick Brown, and the Kyoto and Bloomington Stock Centres for *Drosophila* strains, and Jessica Gamage (née Allen) and Pablo Barrecheguren for their help in the mutagenesis screen.

Competing interests

The authors declare no competing or financial interests.

Author contributions

N.G. conceived the project. J.d.N. designed and performed the mutagenesis screen. J.J. and N.G. performed all other experiments, analysed the data and discussed the results. N.G. wrote the manuscript, with feedback from J.d.N. All authors corrected and approved the final manuscript.

Funding

This work was supported by grants from the Ministerio de Ciencia e Innovación (BFU2011-25828 and a 'Ramón y Cajal' fellowship award) and a Marie Curie Career Integration Grant from the European Commission (PCIG09-GA-2011-293479).

Supplementary information

Supplementary information available online at <http://jcs.biologists.org/lookup/doi/10.1242/jcs.193268.supplemental>

References

- Benjamin, J. M., Kwiatkowski, A. V., Yang, C., Korobova, F., Pokutta, S., Svitkina, T., Weis, W. I. and Nelson, W. J. (2010). AlphaE-catenin regulates actin dynamics independently of cadherin-mediated cell-cell adhesion. *J. Cell Biol.* **189**, 339–352.
- Blanchard, G. B., Kabla, A. J., Schultz, N. L., Butler, L. C., Sanson, B., Gorfinkiel, N., Mahadevan, L. and Adams, R. J. (2009). Tissue tectonics: morphogenetic strain rates, cell shape change and intercalation. *Nat. Methods* **6**, 458–464.
- Blanchard, G. B., Murugesu, S., Adams, R. J., Martínez-Arias, A. and Gorfinkiel, N. (2010). Cytoskeletal dynamics and supracellular organisation of cell shape fluctuations during dorsal closure. *Development* **137**, 2743–2752.
- Borghini, N., Sorokina, M., Shcherbakova, O. G., Weis, W. I., Pruitt, B. L., Nelson, W. J. and Dunn, A. R. (2012). E-cadherin is under constitutive actomyosin-generated tension that is increased at cell-cell contacts upon externally applied stretch. *Proc. Natl. Acad. Sci. USA* **109**, 12568–12573.
- Buckley, C. D., Tan, J., Anderson, K. L., Hanein, D., Volkmann, N., Weis, W. I., Nelson, W. J. and Dunn, A. R. (2014). Cell adhesion. The minimal cadherin-catenin complex binds to actin filaments under force. *Science* **346**, 1254211.
- Butler, L. C., Blanchard, G. B., Kabla, A. J., Lawrence, N. J., Welchman, D. P., Mahadevan, L., Adams, R. J. and Sanson, B. (2009). Cell shape changes indicate a role for extrinsic tensile forces in *Drosophila* germ-band extension. *Nat. Cell Biol.* **11**, 859–864.
- Cavey, M., Rauzi, M., Lenne, P.-F. and Lecuit, T. (2008). A two-tiered mechanism for stabilization and immobilization of E-cadherin. *Nature* **453**, 751–756.
- Chen, C.-S., Hong, S., Indra, I., Sergeeva, A. P., Troyanovsky, R. B., Shapiro, L., Honig, B. and Troyanovsky, S. M. (2015). alpha-Catenin-mediated cadherin clustering couples cadherin and actin dynamics. *J. Cell Biol.* **210**, 647–661.
- Cheng, X., Li, F., Han, S., Zhang, Y., Jiao, C., Wei, J., Ye, K., Wang, Y. and Zhang, H. (2015). Emission behaviors of unsymmetrical 1,3-diaryl-beta-diketones: a model perfectly disclosing the effect of molecular conformation on luminescence of organic solids. *Sci. Rep.* **5**, 9140.
- David, D. J. V., Tishkina, A. and Harris, T. J. C. (2010). The PAR complex regulates pulsed actomyosin contractions during amnioserosa apical constriction in *Drosophila*. *Development* **137**, 1645–1655.
- David, D. J. V., Wang, Q., Feng, J. J. and Harris, T. J. C. (2013). Bazooka inhibits aPKC to limit antagonism of actomyosin networks during amnioserosa apical constriction. *Development* **140**, 4719–4729.
- Desai, R., Sarpal, R., Ishiyama, N., Pellikka, M., Ikura, M. and Tepass, U. (2013). Monomeric alpha-catenin links cadherin to the actin cytoskeleton. *Nat. Cell Biol.* **15**, 261–273.
- Drees, F., Pokutta, S., Yamada, S., Nelson, W. J. and Weis, W. I. (2005). Alpha-catenin is a molecular switch that binds E-cadherin-beta-catenin and regulates actin-filament assembly. *Cell* **123**, 903–915.
- Ellis, S. J., Goult, B. T., Fairchild, M. J., Harris, N. J., Long, J., Lobo, P., Czerniecki, S., Van Petegem, F., Schock, F., Peifer, M. et al. (2013). Talin autoinhibition is required for morphogenesis. *Curr. Biol.* **23**, 1825–1833.
- Fischer, S. C., Blanchard, G. B., Duque, J., Adams, R. J., Arias, A. M., Guest, S. D. and Gorfinkiel, N. (2014). Contractile and mechanical properties of epithelia with perturbed actomyosin dynamics. *PLoS ONE* **9**, e95695.
- Frischmeyer, P. A. and Dietz, H. C. (1999). Nonsense-mediated mRNA decay in health and disease. *Hum. Mol. Genet.* **8**, 1893–1900.
- Gorfinkiel, N. (2016). From actomyosin oscillations to tissue-level deformations. *Dev. Dyn.* **245**, 268–275.
- Gorfinkiel, N. and Martínez Arias, A. (2007). Requirements for Adherens Junctions components in the interaction between epithelial tissues during Dorsal Closure in *Drosophila*. *J. Cell Sci.* **120**, 3289–3298.
- Gorfinkiel, N., Blanchard, G. B., Adams, R. J. and Martínez Arias, A. (2009). Mechanical control of global cell behaviour during dorsal closure in *Drosophila*. *Development* **136**, 1889–1898.
- Gorfinkiel, N., Schamberg, S. and Blanchard, G. B. (2011). Integrative approaches to morphogenesis: lessons from dorsal closure. *Genesis* **49**, 522–533.
- Hara, Y., Shagirov, M. and Toyama, Y. (2016). Cell boundary elongation by non-autonomous contractility in cell oscillation. *Curr. Biol.* **26**, 2388–2396.
- Hazan, R. B., Kang, L., Roe, S., Borgen, P. I. and Rimm, D. L. (1997). Vinculin is associated with the E-cadherin adhesion complex. *J. Biol. Chem.* **272**, 32448–32453.
- Heisenberg, C.-P. and Bellaiche, Y. (2013). Forces in tissue morphogenesis and patterning. *Cell* **153**, 948–962.
- Hutson, M. S., Veldhuis, J., Ma, X., Lynch, H. E., Cranston, P. G. and Brodland, G. W. (2009). Combining laser microsurgery and finite element modeling to assess cell-level epithelial mechanics. *Biophys. J.* **97**, 3075–3085.
- Huveneers, S. and de Rooij, J. (2013). Mechanosensitive systems at the cadherin-F-actin interface. *J. Cell Sci.* **126**, 403–413.
- Imamura, Y., Itoh, M., Maeno, Y., Tsukita, S. and Nagafuchi, A. (1999). Functional domains of alpha-catenin required for the strong state of cadherin-based cell adhesion. *J. Cell Biol.* **144**, 1311–1322.
- Jacinto, A., Woolner, S. and Martin, P. (2002). Dynamic analysis of dorsal closure in *Drosophila*: from genetics to cell biology. *Dev. Cell* **3**, 9–19.
- Kiehart, D. P., Galbraith, C. G., Edwards, K. A., Rickoll, W. L. and Montague, R. A. (2000). Multiple forces contribute to cell sheet morphogenesis for dorsal closure in *Drosophila*. *J. Cell Biol.* **149**, 471–490.
- Kim, T.-J., Zheng, S., Sun, J., Muhamed, I., Wu, J., Lei, L., Kong, X., Leckband, D. E. and Wang, Y. (2015). Dynamic visualization of alpha-catenin reveals rapid, reversible conformation switching between tension states. *Curr. Biol.* **25**, 218–224.
- Kaltschmidt, J. A., Lawrence, N., Morel, V., Balayo, T., Fernandez, B. G., Pelissier, A., Jacinto, A. and Martínez Arias, A. (2002). Planar polarity and actin dynamics in the epidermis of *Drosophila*. *Nat. Cell Biol.* **4**, 937–944.
- Klapholz, B., Herbert, S. L., Wellmann, J., Johnson, R., Parsons, M. and Brown, N. H. (2015). Alternative mechanisms for talin to mediate integrin function. *Curr. Biol.* **25**, 847–857.
- Lecuit, T. and Yap, A. S. (2015). E-cadherin junctions as active mechanical integrators in tissue dynamics. *Nat. Cell Biol.* **17**, 533–539.
- le Duc, Q., Shi, Q., Blonk, I., Sonnenberg, A., Wang, N., Leckband, D. and de Rooij, J. (2010). Vinculin potentiates E-cadherin mechanosensing and is recruited to actin-anchored sites within adherens junctions in a myosin II-dependent manner. *J. Cell Biol.* **189**, 1107–1115.
- Maiden, S. L. and Hardin, J. (2011). The secret life of alpha-catenin: moonlighting in morphogenesis. *J. Cell Biol.* **195**, 543–552.
- Maiden, S. L., Harrison, N., Keegan, J., Cain, B., Lynch, A. M., Pettitt, J. and Hardin, J. (2013). Specific conserved C-terminal amino acids of *Caenorhabditis elegans* HMP-1/alpha-catenin modulate F-actin binding independently of vinculin. *J. Biol. Chem.* **288**, 5694–5706.
- Martin, A. C., Kaschube, M. and Wieschaus, E. F. (2009). Pulsed contractions of an actin-myosin network drive apical constriction. *Nature* **457**, 495–499.
- Meghana, C., Ramdas, N., Hameed, F. M., Rao, M., Shivashankar, G. V. and Narasimha, M. (2011). Integrin adhesion drives the emergent polarization of active cytoskeletal stresses to pattern cell delamination. *Proc. Natl. Acad. Sci. USA* **108**, 9107–9112.
- Mulyil, S., Krishnakumar, P. and Narasimha, M. (2011). Spatial, temporal and molecular hierarchies in the link between death, delamination and dorsal closure. *Development* **138**, 3043–3054.
- Munjal, A., Philippe, J.-M., Munro, E. and Lecuit, T. (2015). A self-organized biomechanical network drives shape changes during tissue morphogenesis. *Nature* **524**, 351–355.
- Narasimha, M. and Brown, N. H. (2004). Novel functions for integrins in epithelial morphogenesis. *Curr. Biol.* **14**, 381–385.
- Pacquelet, A. and Rørth, P. (2005). Regulatory mechanisms required for DE-cadherin function in cell migration and other types of adhesion. *J. Cell Biol.* **170**, 803–812.
- Rauzi, M., Lenne, P. F., Lecuit, T. (2010). Planar polarized actomyosin contractile flows control epithelial junction remodelling. *Nature* **468**, 1110–1114.
- Reed, B. H., Wilk, R., Schöck, F. and Lipshitz, H. D. (2004). Integrin-dependent apposition of *Drosophila* extraembryonic membranes promotes morphogenesis and prevents anokis. *Curr. Biol.* **14**, 372–380.
- Roh-Johnson, M., Shemer, G., Higgins, C. D., McClellan, J. H., Werts, A. D., Tulu, U. S., Gao, L., Betzig, E., Kiehart, D. P. and Goldstein, B. (2012). Triggering a cell shape change by exploiting preexisting actomyosin contractions. *Science* **335**, 1232–1235.
- Ryder, E., Blows, F., Ashburner, M., Bautista-Llacer, R., Coulson, D., Drummond, J., Webster, J., Gubb, D., Gunton, N., Johnson, G. et al. (2004). The DrosDel collection: a set of P-element insertions for generating custom chromosomal aberrations in *Drosophila melanogaster*. *Genetics* **167**, 797–813.
- Sarpal, R., Pellikka, M., Patel, R. R., Hui, F. Y. W., Godt, D. and Tepass, U. (2012). Mutational analysis supports a core role for *Drosophila* alpha-catenin in adherens junction function. *J. Cell Sci.* **125**, 233–245.
- Schuldiner, O., Berdnik, D., Levy, J. M., Wu, J. S., Luginbuhl, D., Gontang, A. C. and Luo, L. (2008). piggyBac-based mosaic screen identifies a postmitotic function for cohesin in regulating developmental axon pruning. *Dev. Cell* **14**, 227–238.

- Solon, J., Kaya-Çopur, A., Colombelli, J. and Brunner, D.** (2009). Pulsed forces timed by a ratchet-like mechanism drive directed tissue movement during dorsal closure. *Cell* **137**, 1331-1342.
- Tepass, U., Gruszynski-DeFeo, E., Haag, T. A., Omatyar, L., Torok, T. and Hartenstein, V.** (1996). shotgun encodes Drosophila E-cadherin and is preferentially required during cell rearrangement in the neurectoderm and other morphogenetically active epithelia. *Genes Dev.* **10**, 672-685.
- Thibault, S. T., Singer, M. A., Miyazaki, W. Y., Milash, B., Dompe, N. A., Singh, C. M., Buchholz, R., Demsky, M., Fawcett, R., Francis-Lang, H. L. et al.** (2004). A complementary transposon tool kit for Drosophila melanogaster using P and piggyBac. *Nat. Genet.* **36**, 283-287.
- Tornavaca, O., Chia, M., Dufton, N., Almagro, L. O., Conway, D. E., Randi, A. M., Schwartz, M. A., Matter, K. and Balda, M. S.** (2015). ZO-1 controls endothelial adherens junctions, cell-cell tension, angiogenesis, and barrier formation. *J. Cell Biol.* **208**, 821-838.
- Toyama, Y., Peralta, X. G., Wells, A. R., Kiehart, D. P. and Edwards, G. S.** (2008). Apoptotic force and tissue dynamics during Drosophila embryogenesis. *Science* **321**, 1683-1686.
- VanHook, A. and Letsou, A.** (2008). Head involution in Drosophila: genetic and morphogenetic connections to dorsal closure. *Dev. Dyn.* **237**, 28-38.
- Vasquez, C. G., Tworoger, M. and Martin, A. C.** (2014). Dynamic myosin phosphorylation regulates contractile pulses and tissue integrity during epithelial morphogenesis. *J. Cell Biol.* **206**, 435-450.
- Wang, Q., Feng, J. J. and Pismen, L. M.** (2012). A cell-level biomechanical model of Drosophila dorsal closure. *Biophys. J.* **103**, 2265-2274.
- Wells, A. R., Zou, R. S., Tulu, U. S., Sokolow, A. C., Crawford, J. M., Edwards, G. S. and Kiehart, D. P.** (2014). Complete canthi removal reveals that forces from the amnioserosa alone are sufficient to drive dorsal closure in Drosophila. *Mol. Biol. Cell* **25**, 3552-3568.
- Yamada, S., Pokutta, S., Drees, F., Weis, W. I. and Nelson, W. J.** (2005). Deconstructing the cadherin-catenin-actin complex. *Cell* **123**, 889-901.
- Yao, M., Qiu, W., Liu, R., Efremov, A. K., Cong, P., Seddiki, R., Payre, M., Lim, C. T., Ladoux, B., Mege, R. M. et al.** (2014). Force-dependent conformational switch of alpha-catenin controls vinculin binding. *Nat. Commun.* **5**, 4525.
- Yap, A. S., Gomez, G. A. and Parton, R. G.** (2015). Adherens junctions revisualized: organizing cadherins as nanoassemblies. *Dev. Cell* **35**, 12-20.
- Yonemura, S., Wada, Y., Watanabe, T., Nagafuchi, A. and Shibata, M.** (2010). alpha-Catenin as a tension transducer that induces adherens junction development. *Nat. Cell Biol.* **12**, 533-542.